

## Spin-glass behavior in iron-aluminum alloys: A microscopic model

Prabodh Shukla and Michael Wortis

Department of Physics and Materials Research Laboratory,  
University of Illinois at Urbana-Champaign, Urbana, Illinois 61801

(Received 9 August 1979)

Drawing upon a model of Sato and Arrott, it is proposed that the spin-glass behavior observed in iron-rich  $\text{Fe}_{1-x}\text{Al}_x$  alloys arises by virtue of competition between a nearest-neighbor Fe-Fe ferromagnetic exchange  $J$  and a further-neighbor Fe-Al-Fe antiferromagnetic superexchange  $-\alpha J$ . The special crystal structure of these alloys makes possible a mapping (decimation) of this model onto a simple-cubic magnet with random exchange. Previous approximate solutions of the simple-cubic model may then be used to construct the  $\text{Fe}_{1-x}\text{Al}_x$  magnetic phase diagram. For an appropriately chosen ratio  $\alpha$  (antiferro/ferro), an acceptable fit to the experimental phase diagram is obtained.

## I. INTRODUCTION

The magnetic behavior of  $\text{Fe}_{1-x}\text{Al}_x$  alloys in the range 0–50 at. % Al has been studied recently by several authors.<sup>1–8</sup> The magnetic phase diagram,<sup>5,8,9</sup> sketched in Fig. 1, shows paramagnetic, ferromagnetic, and spin-glass phases, which meet at a multicritical point in the vicinity of an Al concentration<sup>10</sup>  $x_m \approx 0.295–0.300$  and a temperature  $T_m \approx 90–170$  K. This type of behavior is probably typical of a number of concentrated magnetic alloy systems.<sup>11–13</sup> Unlike "dilute" alloy systems (e.g., dilute CuMn) which have low spin-glass transition temperatures and are believed dominated by long-range Ruderman-Kittel-Kasuya-Yosida (RKKY) interactions, such systems can exhibit quite high transition temperatures and it seems likely that short-range exchange interactions play an important role. Sato and Arrott<sup>14</sup> proposed in

1959 that the disappearance of ferromagnetic order above an Al concentration of  $x = 0.30$  and at sufficiently low temperature  $T$  for  $0.27 < x < 0.30$  is due to competition between nearest-neighbor Fe-Fe ferromagnetic exchange and an indirect Fe-Al-Fe antiferromagnetic superexchange. Their interpretation of the data<sup>1</sup> called for an antiferromagnetic phase at sufficiently low  $T$  for  $0.27 < x < 0.50$ . Neutron scattering<sup>3</sup> failed, however, to reveal the expected antiferromagnetic order, so the model was abandoned. It is now believed that the low-temperature phase for  $0.27 < x < 0.50$  is a spin glass, containing frozen-in moments of all orientations but without long-range order of either ferromagnetic or antiferromagnetic type. Although a full understanding of the spin-glass state is still lacking,<sup>15</sup> there is general agreement that competition between ferromagnetic and antiferromagnetic interactions is required. It is the purpose of this paper to show semiquantitatively that the sort of model proposed by Sato and Arrott<sup>14</sup> can, by appropriate choice of parameters, be made quite consistent with the experimental phase diagram. The particular, detailed choice of interactions in our model is, we emphasize, conjectural and presumably oversimplified: it is certainly not based on any electronic-structure calculations. On the other hand, our principal conclusion—that short-range ferro/antiferro competition can account for the structure of Fig. 1—is, we believe, independent of the details of the model.<sup>16</sup>

Section II describes the model, which is based on the crystal structure of the  $\text{Fe}_{1-x}\text{Al}_x$  system<sup>5,17</sup> and incorporates the observed data on Fe moment formation in alloys.<sup>6</sup> It is an Ising lattice model based on the bcc structure of  $\alpha$ -Fe with inhomogeneity arising from appropriately random siting of the Al atoms. In Sec. III we show how the *site*-random bcc model may be mapped onto a *bond*-random sc model. The phase diagram of this bond-random sc model has

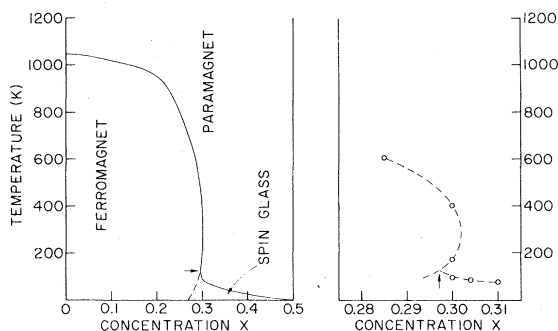


FIG. 1. Magnetic phase diagram for  $\text{Fe}_{1-x}\text{Al}_x$ . Data are taken from Refs. 5, 8, and 9 and include samples with both  $\text{Fe}_3\text{Al}$  and  $\text{FeAl}$  structures (see Sec. II). Shown at right is a detail of the region near the multicritical point,  $x_m, T_m$ , where the paramagnetic, ferromagnetic, and spin-glass phases meet. Data near the multicritical point are not sufficiently good to determine  $T_m$  with precision.

been studied previously by mean-field theory<sup>18</sup> and by various approximate renormalization-group schemes.<sup>19,20</sup> On this basis we calculate in Sec. IV representative  $x, T$  phase diagrams for  $\text{Fe}_{1-x}\text{Al}_x$ . The freedom afforded by the one adjustable parameter  $\alpha$ , which measures the ratio of the strengths of the antiferromagnetic and ferromagnetic interactions, is sufficient to reproduce quite well what is observed in the range  $0.25 < x < 0.50$ . This is the first time to our knowledge that global features of extant theoretical models have been compared to experiment. The approximate theoretical solutions<sup>18-20</sup> on which comparison depends subscribe to the original Edwards-Anderson<sup>21</sup> interpretation of the spin-glass ordering, the details of which are at present controversial<sup>15</sup>; however, in drawing upon them, we take the point of view that global features of the phase diagram are likely to prove insensitive to the details of the ordering.

## II. MODEL

The structure of  $\text{Fe}_{1-x}\text{Al}_x$  alloys is based on the  $\alpha$ -Fe bcc lattice with various Fe atoms replaced by Al. The basic bcc lattice may be regarded as composed of two interpenetrating sc sublattices, which we denote I and II. In stoichiometric FeAl the I sublattice is Fe, while the II sublattice is Al. In stoichiometric  $\text{Fe}_3\text{Al}$  the I sublattice remains pure Fe, but the II sublattice is alternately occupied by Fe and Al in an ordered, rock salt structure. X-ray data show<sup>5,17</sup> that for not-too-high temperatures and for  $0.2 < x < 0.5$  (i.e., except at low Al concentration) the Al in the non-stoichiometric alloys occurs preferentially on sublattice II, while sublattice I remains more or less pure Fe. The full structural phase diagram has been explored by several groups<sup>5,22</sup> and is quite complex. For our purposes it suffices to say that in the spin-glass temperature range the true equilibrium phase shows  $\text{Fe}_3\text{Al}$  order (i.e., long-range alternate order on sublattice II) for  $x \approx 0.25$  and FeAl order (i.e., no long-range alternate order on sublattice II) for  $x \approx 0.5$  but, however, that there is a large concentration range for which stable samples with both  $\text{Fe}_3\text{Al}$  and FeAl order can be prepared by appropriate cooling. Indeed, the data shown in Fig. 1 are composite, including samples with both kinds of order.<sup>8</sup> When samples with different structure but the same overall Al concentration have been compared, no appreciable difference in magnetic properties has been found.<sup>8,17</sup> Thus, it becomes a requirement on any model that  $\text{Fe}_{1-x}\text{Al}_x$  with  $\text{Fe}_3\text{Al}$  and FeAl order should show more or less the same magnetic phase diagram. We shall in what follows treat the  $\text{Fe}_3\text{Al}$  and FeAl orderings slightly differently.

Our model has four ingredients:

*a. Ising variables.* It is assumed that the Fe atoms have localized moments which are describable as Is-

ing variables,

$$\mu_i = m_i \sigma_i, \quad \sigma_i = \pm 1, \quad (1)$$

where  $\mu_i$  is the magnetic moment at the  $i$ th Fe site and  $m_i$  is its magnitude. This approximation is purely practical: theoretical phase-diagram data are only available for Ising systems. It certainly distorts dynamics; we hope that gross thermodynamic features are preserved.

*b. Competing interactions.* Nearest-neighbor Fe-Fe pairs interact via ferromagnetic exchange with an energy  $-J\mu_i\mu_j$ . In addition, any two Fe's which are *sublattice* nearest neighbors interact via antiferromagnetic "superexchange" if they share one or more Al nearest neighbors (on the other sublattice), as illustrated in Fig. 2. The interaction energy is  $\alpha J\mu_i\mu_j$  for each shared Al. Both forms are oversimplified: First, interactions in pure Fe presumably have significant further-neighbor components. Second, superexchange is mediated by atomic electron configurations,<sup>23</sup> and there is no microscopic basis for the postulated angular dependence.<sup>24</sup> In the spirit of the rather crude approximations we shall be forced to make in Secs. III and IV, it might be best to think of the interaction parameters introduced above as "lumped variables." Note that the ferromagnetic and antiferromagnetic interactions are intersublattice and intrasublattice, respectively. If this were the whole story, then stoichiometric FeAl would be antiferromagnetic at sufficiently low temperature, contrary to experiment,<sup>12</sup> which brings us to the next point.

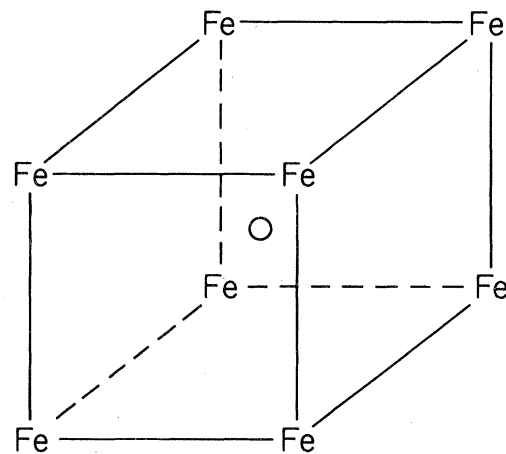


FIG. 2. Model interactions. When the body center is occupied by an Fe atom, there is a ferromagnetic interaction  $-J\mu_i\mu_j$  between the central Fe and its eight nearest neighbors. When the body center is occupied by an Al atom, there is an indirect antiferromagnetic contribution  $\alpha J\mu_i\mu_j$  between each of the twelve Fe-Fe cube-edge pairs. According to our assumptions about Al siting (Sec. II*d*), the cube-corner Fe's are on sublattice I, while the body center is on sublattice II.

c. "Neighbor effect." It is found experimentally<sup>6</sup> that Fe atoms with fewer than four Fe nearest neighbors exhibit magnetic moments dramatically reduced from the  $m_0 = 2.18\mu_B$  characteristic of pure  $\alpha$ -Fe. We write

$$m_i = \gamma_i m_0 . \quad (2)$$

The full dependence of the fractional reduction  $\gamma_i$  on the number  $n$  of Fe neighbors is given in Ref. 6. We use the approximation,

$$\gamma_i = \begin{cases} 1 , & 4 \leq n \leq 8 , \\ 0.27 , & n = 3 , \\ 0 , & n < 3 . \end{cases} \quad (3)$$

Thus, our bcc model Hamiltonian is

$$-\beta\mathcal{H}_{\text{bcc}} = K \sum_{\langle ij \rangle} \gamma_i \gamma_j \sigma_i \sigma_j - \alpha K \sum_{\langle ij \rangle_{\text{Fe-Al-Fe}}} \gamma_i \gamma_j \sigma_i \sigma_j , \quad (4)$$

where

$$K = m_0^2 J / k_B T . \quad (5)$$

The first sum runs over nearest-neighbor Fe-Fe pairs, while the second runs over Fe-Al-Fe sequences, as specified in *b*. It remains to give the positions of the Al atoms.

d. *Randomness.* In accordance with the discussion above, we assume that sublattice I remains pure Fe. This limits the antiferromagnetic interactions in Eq. (4) to Fe atoms on sublattice I. We then have two variants of the model: For alloys with FeAl order we take sublattice II to contain a fraction  $2x$  of Al atoms, randomly sited. For alloys with Fe<sub>3</sub>Al order we modify sublattice II of stoichiometric Fe<sub>3</sub>Al: If  $x > 0.25$ , then a randomly selected fraction  $(4x - 1)$  of the Fe<sub>II</sub> sites are occupied by Al. If  $x < 0.25$ , then a randomly selected fraction  $(1 - 4x)$  of the Al<sub>II</sub> sites are occupied by Fe. These assignments neglect *short-range* compositional order.

### III. DECIMATION

The site-random bcc lattice model set forth in Sec. II can be transformed by "decimation"<sup>25</sup> into an equivalent sc bond-random model by integrating out the degrees of freedom of the Fe atoms on sublattice II. Each unit cube of sublattice I contains a single sublattice II atom, either Fe or Al. Al-centered unit cubes contain only antiferromagnetic interactions between the cube corners [Eq. (4)]. Fe-centered unit cubes contain ferromagnetic interactions which connect the body center only to the cube corners. Thus, in any thermodynamic average the trace over each sublattice II Fe can be carried out independently. This procedure eliminates the sublattice II Fe's but produces new, temperature-dependent effective interactions  $L$  between the sublattice I Fe's on the

corners of the Fe-centered unit cubes, according to

$$\exp \left\{ L^{(0)} + \sum_{\langle ij \rangle} L_{ij}^{(2)} \gamma_i \gamma_j \sigma_i \sigma_j + \sum_{\langle ijkl \rangle} L_{ijkl}^{(4)} \gamma_i \gamma_j \gamma_k \gamma_l \sigma_i \sigma_j \sigma_k \sigma_l + \dots \right\} = \sum_{\sigma_0 = \pm 1} \exp \left\{ K \sum_{l=1}^8 \gamma_l \sigma_0 \sigma_l \right\} , \quad (6)$$

where  $\sigma_0$  refers to the body center and  $\sigma_l$ ,  $\sigma_j$ , etc. are at the corners. Note that further-neighbor and many-spin interactions are generated. Equation (6) is solved by projecting out the desired interactions, for example,

$$L_{ij}^{(2)} \gamma_i \gamma_j = 2^{-8} \text{Tr}_{\sigma} \sigma_i \sigma_j \ln \cosh \left\{ K \sum_{l=1}^8 \gamma_l \sigma_l \right\} , \quad (7)$$

so, when  $\gamma_l = 1$  for all  $l$ ,

$$L_{ij}^{(2)} = L = \frac{1}{128} (\ln \cosh 8K + 4 \ln \cosh 6K + 4 \ln \cosh 4K - 4 \ln \cosh 2K) . \quad (8)$$

Note that the right-hand side of Eq. (7) does vanish, when either  $\gamma_i$  or  $\gamma_j$  vanishes. Generally, the new couplings  $L$  are random through their dependence (via  $\gamma_l$ ) on the random occupation of the cube center and the 26 other sublattice II sites surrounding the cube. Because nearby sublattice I unit cubes share sublattice II neighbors, the interactions  $L^{(n)}$  are not independently random but have some short-range correlation. After all sublattice II Fe atoms have been decimated, we are left with a sc lattice problem with (correlated) random interactions. These interactions are the sum of the original antiferromagnetic interactions (from the Al-centered unit cubes) and the new effective interactions arising from decimation.

We have not carried out the full program described above because it is tediously complicated and leads in the end to a problem with correlated random interactions, including further-neighbor and many-spin interactions, which has not been solved even approximately. In order to be able to make contact with existing solutions, we introduce additional, simplifying approximations which reduce the sc problem to one with uncorrelated nearest-neighbor couplings only,

$$-\beta\mathcal{H}_{\text{sc}} = \sum_{\langle ij \rangle_{\text{nn}}} K'_{ij} \gamma_i \gamma_j \sigma_i \sigma_j , \quad (9)$$

where  $K'_{ij}$  is a sum of contributions from the four unit cubes  $\delta$  which share the edge  $ij$ ,

$$K'_{ij} = \sum_{\delta} K_{\delta} , \quad K_{\delta} = \begin{cases} -\alpha K , & \text{Al-centered cubes} , \\ \frac{7}{3} L , & \text{Fe-centered cubes} . \end{cases} \quad (10)$$

The terms  $-\alpha K$  are just the original antiferromagnet-

ic interactions appearing in Eq. (4). The terms  $\frac{7}{3}L$  represent approximately the indirect ferromagnetic interactions arising from decimation of the Fe-centered cubes. They are obtained as follows: (a) We neglect the many-spin couplings  $L^{(4)}, L^{(6)}$ , and  $L^{(8)}$  generated by Eq. (6). At small  $K$  these go as  $K^4, K^6$ , and  $K^8$ , respectively, so this neglect is certainly justified near the pure ferromagnetic critical point<sup>26</sup>  $K_c$  (bcc) = 0.157. At the lower temperatures of the spin-glass region the approximation is expected to be poorer. (b) There are 28 pair interactions  $L_{ij}^{(2)}$  in each unit cube (12 nearest-neighbor, 12 face-diagonal, and four body-diagonal), each of which may take a number of values between 0 and  $L$ , depending on the  $\gamma_i$ 's (i.e., the cube-corner Fe moments). We replace all these interactions  $L_{ij}^{(2)} \rightarrow L$  (exact at small  $K$ !) and in the spirit of "bond moving"<sup>27</sup> shift them all to the cube edges, producing effective edge bonds of strength  $\frac{28}{12}L$ . This approximation is reasonable for small  $x$  (where most of the  $\gamma_i$ 's are unity) and for  $x \approx 0.5$  (where most of the  $\gamma_i$ 's vanish). It is exact for the  $\text{Fe}_3\text{Al}$  structure with  $x \leq 0.25$ , since there all Fe's have  $\gamma_i = 1$ . Beyond these remarks, we can only point out that the artificial enhancement of ferromagnetism (in the replacement  $L_{ij}^{(2)} \rightarrow L$ ) will to some extent be offset by the loss of *all* interaction when near-neighbor  $\gamma_i \gamma_j = 0$  (but further-neighbor  $\gamma_i \gamma_j \neq 0$ ). The combined effects of dropping higher-order interactions and bond-shifting can be tested directly for the pure ferromagnet ( $x = 0$ ): the nearest-neighbor simple-cubic ferromagnet with coupling  $\frac{28}{3}L$  has a critical temperature  $k_B T_c/J = 6.02$  as compared with the exact bcc result,<sup>26</sup> 6.35. (c) Note, finally, that the correlation of coupling strengths mentioned after Eq. (8) has been lost; however, some correlation between nearest-neighbor moments is still retained in Eq. (9), since the factors  $\gamma_i$  and  $\gamma_j$ , determined via Eq. (3), involve four shared nearest-neighbor sublattice II sites.

#### IV. RESULTS

The random-bond sc models (9) and (10), although not exactly soluble, has been treated approximately via mean-field theory<sup>18</sup> and using position-space renormalization groups.<sup>19,20</sup> Phase diagrams and other data are available from these treatments. We make contact by matching first and second moments of the distribution of coupling strengths  $K_j \gamma_i \gamma_j$ . We can then read off phase-diagram data for our original model (4). Table I gives an idea of the combined effect of all approximations in the purely ferromagnetic limit ( $x = 0$ ). The Southern and Young<sup>19</sup> calculation is seen to give an accuracy of better than 10%. Others are not quite so good. This certainly represents a lower bound on

TABLE I. Critical temperature of the pure ( $x = 0$ ) bcc ferromagnet in various approximations. Decimation reduces  $T_c$  by 5%. Approximation in solving the resulting sc model introduces further inaccuracy.

|   | $k_B T_c/J$ |
|---|-------------|
| Exact bcc <sup>a</sup>                  | 6.35        |
| Decimation plus exact sc <sup>a</sup>   | 6.02        |
| Decimation plus mean field <sup>b</sup> | 7.00        |
| Decimation plus Ref. 19                 | 5.42        |
| Decimation plus Ref. 20                 | 4.19        |

<sup>a</sup>Reference 26.

<sup>b</sup>Reference 18.

the inaccuracies we can reasonably expect for  $x \neq 0$ .

The principal results of the calculation are displayed in Figs. 3 and 4, which show our calculated phase diagrams for  $\text{Fe}_{1-x}\text{Al}_x$  based on the model (4) and using the sc phase diagrams of Refs. 19 and 20, respectively. We have performed calculations for both the  $\text{Fe}_3\text{Al}$  and  $\text{FeAl}$  structures (see Sec. II *d*). The experimental phase diagram (Fig. 1) has been superimposed on all plots for comparison, although the reader is reminded that the actual data points are for  $\text{Fe}_3\text{Al}$  structure, when  $x \leq 0.32$ , and for  $\text{FeAl}$  structure, when  $x \geq 0.32$ , as discussed at the beginning of Sec. II. In constructing Figs. 3 and 4 the overall temperature scale is fixed by the ferromagnetic interaction energy  $J$ , which has been chosen to make the pure-iron Curie point agree with its measured value of 1042 K. The ratio  $\alpha$  of antiferromag-

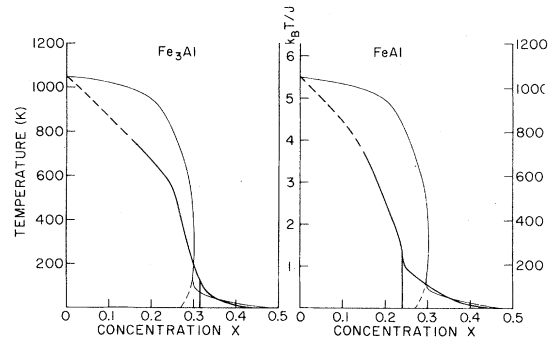


FIG. 3. Calculated magnetic phase diagram of  $\text{Fe}_{1-x}\text{Al}_x$  with (a)  $\text{Fe}_3\text{Al}$  structure and (b)  $\text{FeAl}$  structure, using decimation followed by the Southern and Young (Ref. 19) approximate renormalization group. The experimental phase diagram (shown in thin line) is superimposed for comparison. Note that experimental data is partly for  $\text{Fe}_3\text{Al}$  structure ( $x \leq 0.32$ ) and partly for  $\text{FeAl}$  structure ( $x \geq 0.32$ ). The ferromagnetic coupling  $J$  is chosen to make the pure-iron Curie temperature agree with experiment. Both graphs correspond to  $\alpha = 0.14$ , which is chosen to make  $T_m$  ( $\text{Fe}_3\text{Al}$ ) coincide with experiment.

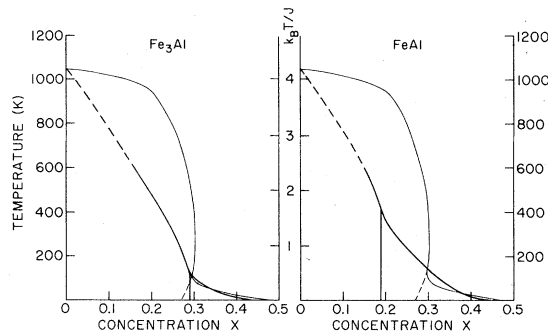


FIG. 4. Calculated magnetic phase diagram of  $\text{Fe}_{1-x}\text{Al}_x$  with (a)  $\text{Fe}_3\text{Al}$  structure and (b)  $\text{FeAl}$  structure, using decimation followed by the Jayaprakash *et al.* (Ref. 20) approximate renormalization group. See Fig. 3 caption for comments. Here  $\alpha = 0.38$ .

netic to ferromagnetic interaction strength remains at our disposal. It turns out that the multicritical temperature  $T_m$  is quite sensitive to  $\alpha$ , while the multicritical concentration  $x_m$  is exceedingly insensitive.<sup>28</sup> We have in all cases chosen  $\alpha$  to fix  $T_m$  for the  $\text{Fe}_3\text{Al}$  structure at its experimental value.<sup>10,29</sup> We find  $\alpha = 0.14$  (Southern and Young, Ref. 19) and  $\alpha = 0.38$  (Jayaprakash *et al.*, Ref. 20), which are not physically unreasonable. Once  $J$  and  $\alpha$  are set, everything else is determined. In particular,  $x_m$  and  $x_0$  (the  $T = 0$  boundary between the ferromagnet and the spin glass) are predicted by the calculation in reasonable agreement with experiment. Furthermore, we use the  $\alpha$  determined for the  $\text{Fe}_3\text{Al}$  structure to compute the  $\text{FeAl}$ -structure phase diagram; so it is an output of the model that the two phase diagrams are similar. The overall pattern of reasonable agreement with experiment lends credence to the proposed model. We close with two more-detailed remarks.

The experimental ferromagnetic phase boundary shows a "recurved" behavior: for  $0.28 < x < 0.30$  ferromagnetism at high temperature gives way, as the temperature is lowered, to spin-glass behavior.<sup>30</sup> Indeed, there is even a region  $x_m < x < 0.30$  where the paramagnetic phase intervenes between the two. Although our calculated ferromagnet-paramagnet phase boundary is *not* recurved, it does show a marked steepening near  $T_m$ . Furthermore, our ferromagnet-spin-glass phase boundary is actually very slightly recurved (i.e.,  $x_0 < x_m$ ).

The most notable failure of the model is in the strongly ferromagnetic region  $0 < x < 0.2$ , where experiment shows a markedly higher transition temperature than the model predicts. We cannot explain this failure; however, there are several reasons why the model may be poor in this region. The structural assumption (Sec. II *d*) that Al atoms are restricted to sublattice II sites must clearly fail for small  $x$ . The replacement of Heisenberg spins by Ising variables is most suspect for low  $x$ , where the coherence of spin-wave excitations is not yet strongly broken up by the percolative influence of the Al impurities. Finally, if weak but long-range ferromagnetic interactions (neglected in our model) are present, then it is just in this region that they should be most strongly felt: the spin disorder at higher  $x$  will tend to average out the effect of longer-range interactions.

#### ACKNOWLEDGMENTS

We thank Professor Paul Beck for many stimulating and informative conversations. We acknowledge with thanks support from NSF Grants No. DMR 77-23999 and No. DMR 78-21069. One of us (M.W.) is grateful for the hospitality of the Brookhaven National Laboratory. We thank Dr. G. Grest for providing us with a prepublication copy of his work.

<sup>1</sup>A. Arrott and H. Sato, Phys. Rev. **114**, 1420 (1959).

<sup>2</sup>J. S. Kouvel, J. Appl. Phys. Suppl. **30**, 313S (1959).

<sup>3</sup>S. J. Pickart and R. Nathans, Phys. Rev. **123**, 1163 (1961).

<sup>4</sup>A. Olés, Acta Phys. Pol. **27**, 343 (1965).

<sup>5</sup>H. Okamoto and P. A. Beck, Metall. Trans. **2**, 569 (1971).

<sup>6</sup>P. A. Beck, Metall. Trans. **2**, 2015 (1971).

<sup>7</sup>G. P. Hoffman, J. Appl. Phys. **42**, 1606 (1971).

<sup>8</sup>R. D. Shull, H. Okamoto, and P. A. Beck, Solid State Commun. **20**, 863 (1976).

<sup>9</sup>M. Hansen and K. Anderko, *Constitution of Binary Alloys* (McGraw-Hill, New York, 1958), p. 93.

<sup>10</sup>In the crucial region near the multicritical point there are only six data points.  $x_m$  is determined quite well;  $T_m$ , quite poorly. For working purposes we adopt  $x_m = 0.297$ ,  $T_m = 127$  K.

<sup>11</sup>J. A. Mydosh, in *Proceedings of the 20th Conference on Magnetism and Magnetic Materials, San Francisco, 1974*, edited by C. O. Graham, Jr., G. H. Lander, and J. J.

Rhyne, AIP Conf. Proc. No. 24, (AIP, New York, 1975), p. 131.

<sup>12</sup>A. Parthasarathi and P. A. Beck, Solid State Commun. **18**, 211 (1976).

<sup>13</sup>P. A. Beck, Prog. Mater. Sci. **23**, 1 (1978).

<sup>14</sup>H. Sato and A. Arrott, Phys. Rev. **114**, 1427 (1959).

<sup>15</sup>P. W. Anderson, in *Amorphous Magnetism II*, edited by R. A. Levy and R. Hasegawa (Plenum, New York, 1977), p. 1.

<sup>16</sup>In a companion paper to this one, G. Grest, Phys. Rev. B **21**, 165 (1980) (following paper) treats a model similar to ours but incorporating the antiferromagnetic superexchange in a somewhat different way. He uses a Monte Carlo method and obtains results which at a qualitative level are identical to ours.

<sup>17</sup>P. A. Beck (private communication).

<sup>18</sup>D. Sherrington and S. Kirkpatrick, Phys. Rev. Lett. **35**, 1792 (1975).

<sup>19</sup>B. W. Southern and A. P. Young, J. Phys. C **10**, 2179 (1977).

- <sup>20</sup>C. Jayaprakash, J. Chalupa, and M. Wortis, *Phys. Rev. B* 15, 1495 (1977).
- <sup>21</sup>S. F. Edwards and P. W. Anderson, *J. Phys. F* 5, 965 (1975).
- <sup>22</sup>H. J. McQueen and G. C. Kuczynski, *Trans. Metall. Soc. AIME* 215, 619 (1959). S. M. Allen and J. W. Cahn, *Acta Metall.* 23, 1017 (1975); 24, 425 (1976); *Scr. Metall.* 10, 451 (1976); S. M. Allen, *Philos. Mag.* 36, 181 (1977).
- <sup>23</sup>N. W. Ashcroft and N. D. Mermin, *Solid State Physics* (Holt, Rinehart and Winston, New York, 1976), p. 681.
- <sup>24</sup>In Ref. 16 it is assumed that the Fe-Al-Fe sequence should be colinear, i.e., along a body diagonal.
- <sup>25</sup>L. P. Kadanoff and A. Houghton, *Phys. Rev. B* 11, 377 (1975).
- <sup>26</sup>*Phase Transitions and Critical Phenomena*, edited by C. Domb and M. S. Green (Academic, New York, 1974), Vol. III.
- <sup>27</sup>L. P. Kadanoff, *Ann. Phys. (N. Y.)* 100, 359 (1976).
- <sup>28</sup>Increasing  $\alpha$  for the  $\text{Fe}_3\text{Al}$  structure in the approximation of Ref. 19 from 0.14 to 0.20 decreases  $k_B T_m / J$  from 0.67 to 0.60 but only decreases  $x_m$  from 0.3152 to 0.3147.
- <sup>29</sup>Note that the experimental data near the multicritical point are for the  $\text{Fe}_3\text{Al}$  structure.
- <sup>30</sup>The data in this region (Ref. 8) are exceedingly sensitive to the presence of small magnetic fields (Ref. 17).